

Assessment of the performance of conventional spray models under high pressure and temperature conditions using a “Design of Experiments” approach

Daniel M. Nsikane¹, Konstantina Vogiatzaki¹, Robert Morgan¹, Morgan Heikal¹

¹ Advanced Engineering Centre, University of Brighton, United Kingdom²

Abstract

An integrated Design of Experiments (DoE) with Reynolds Averaged Navier Stokes (RANS) approach is suggested and implemented to model turbulent spray combustion. In the automotive industry, DoE is often combined with an optimizer and is used to find an optimum set of internal combustion engine calibration parameters for set criteria at reduced experimental effort. The novelty of the numerical approach suggested here, is that the methodology is adjusted to provide an optimal set of model “tuning constants” for the 3D CFD simulations which best matched experimental data at three conditions taken from the Engine Combustion Network (ECN) database. Multi-variable DoE were run for each condition. The goal of this work is to use these DoE derived coefficient sensitivities and link the observed trends to real physical processes. The analysis is based on both microscopic (droplet statistics) and macroscopic (liquid & vapor penetration and heat release) spray characteristics. Results indicate that a single coefficient matrix exists that can model a wide range of injection pressures. This finding is important since it paves the way for using conventional spray models for high pressure injection conditions, if tuned appropriately. Moreover, a separation of the model coefficients between the ones that affect mostly non-reactive predictions and the ones that affect reactive cases is suggested. This reduces the computational cost of the suggested methodology since the reactive DoE can be restricted on a sub-set of coefficients. The physical meaning of these coefficient groups reveals the link between the various sub models when turbulence and evaporation are the only processes acting on the droplets as well as when these processes are coupled with combustion.

Keywords: Spray, atomization, drop size analysis, Design of Experiment

Introduction

With the automotive sector facing growing challenges to meet tightening emission regulation standards for internal combustion engines (ICE) at shortening development cycles, the importance of early stage numerical simulation for in-cylinder processes is growing. Simulating the full spray combustion process from injection to combustion, in particular for realistic conditions (injection pressures reaching up to 300MPa), is extremely challenging and a computationally demanding task. Due to the multi-scale, multi-phase nature of liquid–gas interactions and the complexity of finite-rate evaporation, mixing and multi-step reactions, an “all scale analysis” (Direct Numerical Simulations (DNS)) is impossible with the current numerical capabilities. Large-Eddy Simulation (LES) models are expected to be more appropriate for turbulent spray combustion and have indeed attracted the interest of the scientific community. However, for industrial purposes, the computational cost of these techniques remains high and most LES studies of realistic geometries constitute under resolved LES simulations, especially in respect to the smallest scales of the multiphase nature of the flow[1, 2]. Up to now, due to its favorable simulation durations, the chosen method in the majority of industrial environments is typically RANS[3]. RANS applies an averaged statistical approach in which the prediction of various fluctuating quantities of interest are numerically triggered based on sub grid scale (SGS) models. The advantage is that through this scale averaging, computational cost is low but the profound disadvantage being that the predictive character of such methods becomes strongly dependent on the performance of the SGS models.

Apart from the accurate selection of the appropriate sub-models, another challenging issue is the selection of the model constants. These parameters are used by modelers to numerically tune the models and the fact that they physically encapsulate “unknown” or “unresolved” information at the sub grid scales is sometimes overlooked. Determining which coefficients have a significant impact on performance measures of interest can be a daunting task. The common approach of changing one factor at a time is very often incorrect and misleading, because many model constants interact and impact on the responses. As a result, it is unclear if the accuracy of the presented results in the literature is indicative of the good model performance in terms of physical representation or the result of coefficient tuning and/or code numeric. The above issue is of importance when Computational Fluid Dynamics (CFD) are used to guide the design of novel systems that operate outside the conventional thermodynamic framework. For example, for low pressure injection cases, many studies have already been performed in the 80s and 90s. A general consensus exists on which model values should be used, especially for the standard $k-\epsilon$ and $k-\epsilon$ RNG turbulence models [4]. When the injection pressure is increased three important questions arise:

a) Is there a coefficient matrix for the various sub-models used in spray combustion (namely turbulence, atomization, evaporation, turbulent flame speed) that can provide good match with experimental data corresponding to trans critical conditions? This question can help us understand if the conventional models are appropriate for high pressure injection cases subject to sophisticated tuning.

b) If this coefficient matrix exists, is it also applicable to a wide range of injection pressures? This question is related to the fact that models which require minimum tuning to perform well under wide operating conditions are needed. Otherwise the predictive character of CFD is lost.

c) If the model is tuned based on non-reactive conditions, can the same tuning coefficients be used for reactive conditions? The answer to this final question can also be linked to the question whether accurate mixture formation prediction under high pressure injection conditions controls predictions for the combustion phase.

Initial work towards answering the first question has been performed by the authors in [5]. This work is an extension of the previous publication to cover the second and third question. The paper is structured as following: In Section two the main components of the methodology are briefly introduced. Broadly, this is based on an integration of the Design of Experiment approach (DoE) with Eulerian/Lagrangian RANS calculations. In Section three, non-reactive calculations for liquid and vapor penetration (LP & VP) are presented. In comparison to [5], the focus here is shifted from the best match confined matrix towards defining a matrix that is suitable in modelling a wide injection pressure range. In Section four, the matrix for coefficients associated with mixture preparation along with the matrix for coefficients relevant to combustion is used to examine to what extent mixing controls combustion under high pressure conditions. Finally, conclusions and suggestions for future work are presented. The goal of this work is to use these DoE derived coefficient sensitivities and link the observed trends to real physical processes. An analysis based on the microscopic spray characteristics (droplets statistics) is also performed to explain the findings relevant to the macroscopic quantities (LP and VP and HR).

Methodology

Experimental and Numerical Set up

The dataset used for validation in this paper is commonly known as the ECN's Spray A (see Table 1). The diesel surrogate n-dodecane is injected vertically through a single hole injector into a quiescent high pressure, elevated temperature vessel. The boundary conditions have been extensively reported in [6-8] while additional information for the experimental setup and the data acquisition process is thoroughly reported in [9-11]. The ECN Spray A has also been the basis of other validation studies [12, 13]. The novelty of this work lies in the fact that a rigorous and systematic approach to understanding the coefficient sensitivities with regard to the boundary condition has become the basis for automated or tabulated simulation tuning.

Table 1: ECN Spray A nominal conditions

Case	Charge Temperature (K)	Charge Density (kg/m ³)	Inj. Pressure (MPa)	Reactive (Yes/No)	No. Simulations	Duration per Simulation (hrs)
1	900	22.8	150	No	100	2
2			100			
3			50			
4			150	Yes		

The conditions described in Table 1 were simulated using Ricardo Software's commercially available VEC-TIS CFD package which is a well-validated code with a long history of extensive industrial use for ICEs [14]. A RANS framework was used with the standard k-ε model turbulence model[4]. The liquid fuel was introduced using the "blob" method and tracked with an Eulerian-Lagrangian method. When injected, the droplets experience drag forces, which were approximated using the Putnam drag model[15]. The breakup process as the droplets travel through the domain was calculated with the well-established KH-RT hybrid breakup model [16, 17]. As the droplets travel through the domain they experience droplet evaporation which was approximated following the Spalding correlation [18, 19]. Droplet-droplet (collision and coalescence) as well as droplet-turbulence models included phase interaction effects in two-way coupling. In the reactive case, Ricardo's Two-Zone Flamelet (RTZF) model [20] was used to simulate the combustion. Laminar flame speed was defined by the modified Metghachi & Keck model [21] while turbulent flame speed followed the Gülder equation [22]. As reported in the previous work [5], mesh, time step and parcel rate introduction rate independence studies were conducted. The traditional approach of reducing mesh size in runs with otherwise identical numerical set up suggested an independent mesh at a cell size of 0.45mm. The inert case domain where run as a section of cube with 817667 cells, while the reactive cases were run on the full geometry counting 1017485 cells. Similar grid sizes are reported amongst other ECN participants, increasing the level of confidence[23]. A parcel introduction rate (PIR) study was performed, which showed no benefit to increasing this beyond 3.6 million per second.

Design of Experiments approach

Due to the multivariable interactions of tuning factors, discretely changing them between conditions does not reveal their real connection. In this work, an integrated DoE/RANS approach is used to assess the substantial number of coefficient combinations with low computational cost. The DoE approach has been implemented extensively in experimental context in the past as well as means of selecting chemical mechanisms more recently

in[24, 25]. In the current work, the method was modified to suit the purpose of investigating computational simulations for spray combustion. The experiments are replaced by simulation runs, input parameters substituted with sub model tuning constants and the output parameters are defined as the calculated root-mean-square-errors (RMSE) between the experimental and simulated characteristics. This approach can visualize the complex interactions between key simulation constants which influence certain metrics of the simulation. Especially useful is that the error (difference between the simulated and experimental values) is quantifiable. Using the DoE approach, the influence of various parameters shown in Table 2 was investigated. The physical context of these coefficients is indicated in the third column. While the DoE conducted for the reactive case included all variables, the DoE for the inert cases excluded the block of variables under the ‘combustion coefficients’ group and C_1 . The suggested grouping should not be considered as strict since turbulence, combustion and spray dynamics are all interlinked. However, it is useful in the interpretation of the results. Based on the which coefficients needed to be adjusted for each pressure swing it can identified which physical processes increase in importance as the injection pressure increases.

Table 2: List of DoE variables, their set ranges and default values for the three inert cases

Parameter	Range	Phenomenon	Group
Schmidt Number	0.6 – 1	Species Diffusivity	Turbulence Coefficients
Coefficient of Dissipation C_1 (-)	1.35 – 1.55	Production of Turbulence	
Coefficient of Dissipation C_2 (-)	1.65 – 1.9	Destruction of Turbulence	
Burning Velocity Coefficient (-)	0.3 – 1.5	Combustion	Combustion Coefficients
Auto-Ignition Coefficient (-)	0.3 – 1.2	Ignition	
Turbulent Flame Speed Multiplier (-)	0.1 – 3	Turbulent Combustion	
Drag scaling factor A_{drag} (-)	0.2 – 1.5	Momentum Transfer	Droplet Breakup Coefficients
KH B_1 – Constant (-)	1 – 40	Primary Atomization	
KH B_0 – Constant (-)	0.3 – 0.8	Primary Atomization	
RT CRT – Constant (-)	0.3 – 2	Secondary Atomization	
RT - C_3 – Constant (-)	0.3 – 5.3	Secondary Atomization	
Levich Abu – Constant (-)	5 – 12	Primary/Secondary Atomization	
Initial droplet diameter D_0 (μm)	60 – 90	Droplet Introduction	Initial conditions
Initial Half Cone Angle α_{cone} (deg)	2.5 – 7.5	Initial Dispersion	

A detailed description of the role of the combustion and turbulence parameters is given below. The reader can find a summarized description of the KH-RT breakup model in the author’s preceding publication [5] or refer to the original documentation for a detailed description [16, 17].

In the standard k- ϵ turbulence model, the coefficients C_1 and C_2 adjust the generation and destruction rate of turbulence kinetic energy and turbulent dissipation. Through variation in the coefficient values it is possible to adjust the transport of both k and ϵ as shown in equation (1).

$$\frac{\partial(\rho\epsilon)}{\partial t} + \frac{\partial(\rho U_i \epsilon)}{\partial x_i} = \frac{\partial}{\partial x_i} \left[\left(\mu_L + \frac{\mu_t}{\sigma_{\epsilon-1}} \right) \frac{\partial \epsilon}{\partial x_i} \right] + \frac{\epsilon}{k} \left(C_1 G - C_2 \rho \epsilon + C_3 \rho k \frac{\partial U_i}{\partial x_i} \right) \quad (1)$$

The Schmidt number affects the species mass transport process and is considered in both the species and energy transport equations. The RTZF combustion model solves a transport equation for each species with the source terms determined by the generalized burning rate that can account for both pre-mixed and non-premixed modes. In the case of non-premixed such as this the generalized burning rate is determined from the combination of the auto-ignition model burning rate (Livengood-Wu model) and the turbulence controlled burning rate. In the Livengood-Wu model, the low-temperature reactions for auto-ignition are considered as a lumped one-step reaction of one generic intermediate ignition species, which is inversely proportional to the ignition time t_{ig} . The fuel reactant coefficient c_{ig} linearly alters ignition delay which in physical terms accounts for reaction rates of the fuel. The single ignition delay coefficient is therefore well suited for the multi-variable optimization process. The correlation is shown in eq. (2) where P_{ig} is the probability of reactant autoignition.

$$P_{ig} = c_{ig} \int \frac{dt}{t_{ig}} \quad (2)$$

The RTZF is capable of simulating both non-premixed and pre-mixed combustion and hence utilizes a turbulent flame speed calculation in the generalized burning rate calculation. In the case of non-premixed combustion, the turbulent flame speed has limited but non-negligible contribution in determining this rate and was considered in this case. The reason is that although spray combustion is predominately non- pre-mixed, there might be areas where also premixed behavior is noticed, especially further downstream as noticed in previous publications [26]. The burning velocity coefficient A_0 is a direct multiplier in the reaction source terms (Eq. (3)). The turbulent burn

rate is further dependent on the ratio between fully mixed reactant to the total volume r_{vol} , unburned-zone density ρ_u , the turbulent Schmidt number S_t and the length scale l_c .

$$\omega_f = \frac{A_0}{l_c} r_{vol} \rho_u S_t C (1 - C) \quad (3)$$

The turbulent flame speed coefficient α scales the turbulent flame speed using Gülder equation. As shown in Eq. (4), the turbulent flame speed S_P is a function of laminar flame speed S_L , turbulence intensity u' and α . In this work only the influence of α while the rest of the coefficients are selected based on previous studies is investigated. For α , a value close to 0 would minimize the effect of turbulence on the flame speed while increasingly higher values increase the effect of turbulence on the flame speed.

$$\frac{S_P}{S_L(\phi)} = 1 + \alpha \left(\frac{u'}{S_L(\phi)} \right)^q \quad (4)$$

The steps followed for the DoE preparation are the following:

Simulation Matrix: Separate DoE's are run for the inert and reactive cases. Every key point was assigned with an individual combination of the parameters within the ranges shown in Table 2. To achieve statistical relevance for the stochastic process model, 10 simulations were run per variable shown in Table 2. Therefore, a total of 100 simulations were run for each of the three inert cases (10 coefficients) and 140 simulations for the single reactive case (14 coefficients). The average duration per simulation on 20 cores Intel(R) Xeon(R) CPU E5-2650 v3 CPUs with 2.30GHz was around 2hrs of the inert and 7hrs for the reactive cases.

Stochastic Process Model: A stochastic process model (SPM) is a multidimensional correlation between inputs and outputs, allowing to study the effects of input parameters, which are not included in the original input matrix, on the output.

Optimizer: Finally, an optimizer uses the SPM to find a combination of input parameters that minimize the difference between simulated and experimental curve propagations of pre-specified quantities. For the inert cases, the vapor and LP were used as optimization criterion for the correct mixture fraction distribution. In the reactive case, in addition to LP and VP, the HR was selected as it will be an important combustion criterion for both emission and performance predictions in future work. As a quality measure between the measured and simulated curves, the root-mean-square-error (RMSE) across the steady state of the spray injection was calculated. As all RMSE's could never simultaneously be zero, the optimizer produced a pareto diagram showing trade-offs of settings for the user to choose from.

Results and Discussion

Inert Spray A

Three injection pressures were used for the simulations, 150,100 and 50MPa. The process leading up to the finding of the best match for each of these cases is described in more detail in [5]. The outcomes of this work indicated that given appropriate tuning, a separate set of coefficients could indeed be found to tune the model for every different case. The hardest one to tune was the 50MPa case, where the importance of the turbulence coefficient C_2 and liquid-to-gas phase coupling in form of the drag scaling factor A_{drag} and droplet sizes was indicated. Our initial focus in this section was to investigate whether a single set of constants could match all three boundary conditions. The results of this study are shown in Fig. 1. Experimental LP and VP profiles over time for the three different pressures and compared with numerical simulations from the integrated DoE/RANS approach. The LP was defined as the axial location where 99% of the total droplet mass stays in the upstream side. The VP was determined by the farthest downstream location of 0.1% fuel mass fraction. In all the simulation cases, the same values for the set of coefficients shown in Table 2 were used.

For all three cases, a good match was achieved with a single set of coefficients (indicated in the figure as "Cross Case Best Match"). In Case 3 a small discrepancy at the initial stages (0.5-1.5ms) of the VP was noticed. In all three cases the experimental LPs are almost identical (~10mm), a trend that was well reproduced by the simulations. The experimental VP appears to be more sensitive to falling injection pressure with Case 3 showing a lower VP across the 4ms range. This is an indication of lower momentum transfer from liquid to vapor, which is associated with the individual droplet size distributions in each case. The simulated VPs captured this trend well. One factor of importance in the spray penetration process is the influence of evaporation. It is expected that lower injection pressures allow for generally larger droplets to be created. Larger droplets tend to evaporate slower and thus travel longer. Another effect that must be considered and might counteract the evaporation effect is the initial inertia of the jet based on the injection pressure. Previous studies [27] have shown that small droplets carry less inertia of the initial spray momentum. This makes them more prone to the strong turbulent gas motion created as a result of drag effects and the kinetic energy of the evaporated fuel. For the three cases under consideration, it is hard to quantify this effect since Case 3, because of the lower injection pressure, imposes less initial momentum than Case 1. At the same time, the droplets are expected to be larger than Case 1 which means they carry more of

the initial momentum than in Case 1. This might explain the fact that although the LP remains the same in all three cases (the smaller droplet size counterbalances the larger initial momentum imposed by the higher pressure), because of their varied sizes they evaporate in a different rate which explains the lower VP in Case 3.

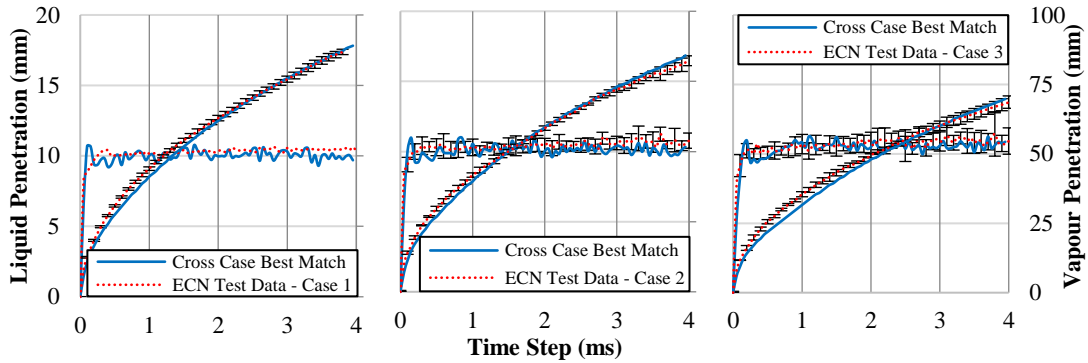


Figure 1: Comparison of LP and VP between ECN test data and simulation cases 1, 2 and. Error bars are at 2σ confidence. For the LP in Case 1 there are no error bars available on the ECN website.

Figure 2a, shows that the Probability Density Function (PDFs) of the droplet sizes at 2mm (near the nozzle) are identical. This is an expected effect of the blob methodology used to simulate droplet injection. Further downstream they begin to differ. At 5mm the higher injection pressure case presents larger droplet sizes than the other two cases. Also, the distribution is wider. One explanation for this could be that because of the higher injection pressure, the injected droplets have a higher axial velocity and therefore cover more distance before disintegrating into smaller droplets. However, at 9mm after the nozzle exit, the droplet sizes of the higher injection pressures are smaller than shown in Case 3. This is an indication that over the distance covered between 5 and 9mm the droplets have broken up faster. To confirm the previous statement, Figure 2b, is included which shows the droplet evolution. Their size in the figure is analogous to their diameter while the coloring shows the temperature contour. In all cases, primary atomization is completed at ~ 7 mm. While in Case 3, larger droplets are seen to linger in greater numbers, Case 1 and 2 show signs of rapid secondary breakup. It is a characteristic of high pressure sprays to exhibit this kind of behavior[28].

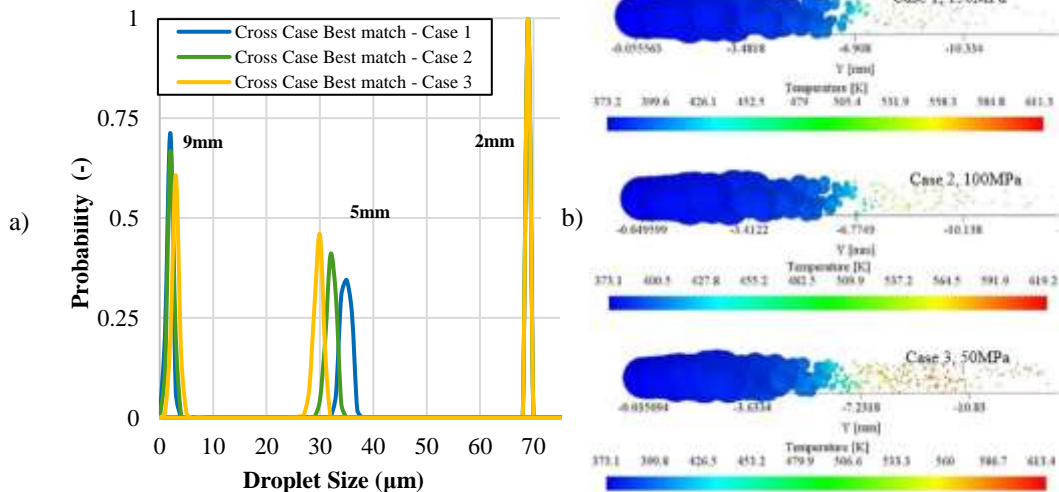


Figure 2: Droplet size distributions of the simulations of cases 1, 2 and 3 at 2, 5 and 9mm distance to the nozzle exit (a) and droplet evaporation and break up process shown based on droplet mean diameter and temperature (b)

DoE on reactive Spray A

This section focusses on the question whether a simulated spray that was well tuned to match experimental data under inert conditions also leads to a good correlation under reacting conditions. Cases 1 and 4 from Table 1 were the basis for this investigation. More specifically, the DoE for this reactive case contained all parameters as in the previous non-reactive case and included relevant turbulent chemistry interaction, ignition and combustion parameters shown in Table 2. The goal was to observe which coefficients a full-scale DoE and subsequent optimization would produce a matching simulation. Based on the outcome, it could be seen which coefficients must change between the reacting and non-reacting case.

Figure 3 is a visualization of the design space and allows us to give a more physical explanation of the selected coefficient values that resulted from the DoE. The physical quantities used as base indicators for error minimization are VP, LP, total HR and Lift-off-Length (LoL), and are each represented in the four rows. Every column represents the error response of one of the investigated DoE constants within their given ranges. A trend of the curve indicates the increase or decrease of the error between the experimental and simulated data. The dashed lines above and below the solid line indicate response uncertainties of 2σ standard deviation. In the figure, the coefficients have been grouped according to their significance for the various phenomena taking place (turbulent motion, spray breakup, combustion etc.) following Table 2. Although this separation is not strict because the mutual interaction of all these processes cannot be ignored, the separation allows us to provide a map between physical phenomena and the values of the coefficients. In the VP error row, it is apparent that turbulence dissipation coefficients C_1 and C_2 are the defining parameters to match the vapor curve. Similarly, in the case of HR, the SPM shows it to be only sensitive to the diffusion, dissipation, turbulent combustion and burn velocity. Finally, the last row shows that the LoL is mainly dependent on the KH-RT spray breakup time scales B_1 and C_3 and the Levich switching criterion A_{bu} . The former coefficients play an important role in the breakup timescale of the droplets while the latter defines the location at which the KH-RT model switches between primary and secondary breakup considerations. Hence, these coefficients are responsible for droplet shrinking. Further, the reactant autoignition coefficient c_{ig} influences the error. This makes sense, as manually increasing or decreasing the probability of autoignition plays an important role in the spatial and temporal Start of Combustion (SOC). The relationship between the location of droplet evaporation and autoignition yields the lift-off-length. At this point it is important to highlight the assisting roles of the LP and lift-off-length error. There are no LP measurements for the reactive case handled in this work. However, in research by [9] it is suggested that the LP is insensitive to downstream combustion and HR effects. Therefore, it was justified to use the LP from the inert 900K as a reference point for the LP under reacting conditions. Usually when investigating reactive sprays, the LoL and ignition delay play a major role in assessing the quality of simulations, but due to the simplicity of the used models (no detailed chemistry), it was not possible to compare the quantities delivered by the ECN. Therefore, lift-off-length is only a qualitative comparison metric for assessment of the results.

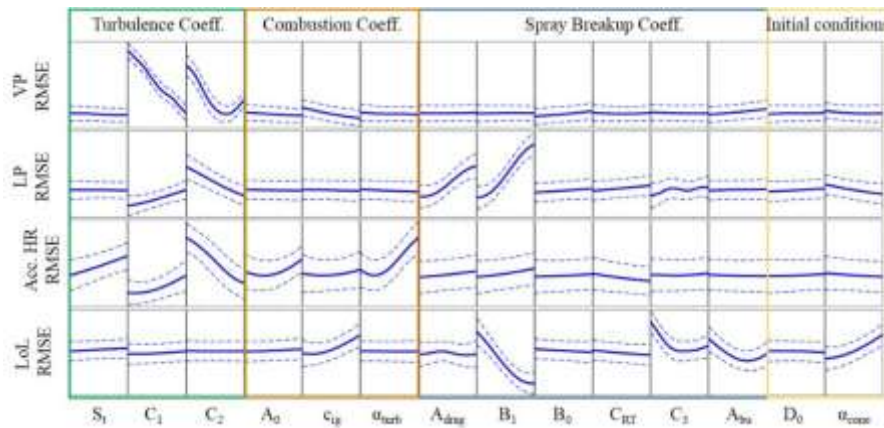


Figure 3: Stochastic Process Model (SPM) showing error sensitivity of all 14 variables within their ranges

Next, the model was ran through the optimizer. As well as other theoretical combinations, the optimizer suggested a combination of constants similar to the constants used in the inert cases. While most other combinations were capable of matching one or two target metrics, only the constant matrix resembling the inert case breakup constants matched all metrics to a satisfying standard and additionally produced a reasonable LP of around 11 mm (see Figure 4, ‘Optimized simulation’, green).

Since, LP measurements do not exist for the reactive case, the simulated LP is was compared to the inert LP of Case 1. To indicate that this is a qualitative comparison, the curve is grayed out. The reactive spray penetration was compared from the time of SOC. Figure 4 shows that the simulated reactive vapor plume follows the trend well, however lags the experimental values. The SPM in Figure 3 shows that the error between LP and VP is a tradeoff leading to the shown solution being the best combination. Since the breakup constants were very similar between the inert and reactive cases and combustion coefficients and turbulent Schmidt number had little to no effect on the liquid and vapor characteristics (Figure 3), it can be conclude that the increase of vapor propagation between the inert and reactive sprays (~6mm at 3.5ms orange and red dashed lines) stems from the new turbulence coefficients C_1 and C_2 . These new turbulence coefficients were significantly higher than in the inert ‘best match’ from Figure 1. Based on this finding, it can be concluded that when transferring a simulation set up from an inert to reactive case, initial conditions and liquid breakup setup can be fixed, as they are not affected by downstream combustion. The turbulent gas motion however, must be adjusted to account for combustion induced turbulent

motion. The fact that with this increased turbulent motion comes an increased mismatch of LP suggests that the turbulent coefficients C_1 and C_2 are not able to replicate liquid and vapor motion simultaneously across the whole domain and opens room for the question of temporal and spatial variable or tabulated C_1 and C_2 values.

On the right side of Figure 4 instantaneous and accumulated HR are shown. Except a mismatch at the early stages of ignition, both trends are captured well. The reason the distinct initial HR spikes were not captured was that in the simulations the simple Livingood-Wu autoignition model was used, which is not capable of identifying local combustion events and/or flame extinction. Despite the mismatch of the spikes, the rise of HR indicating the SOC and the steady state burn are captured well.

Finally, the values in the droplet breakup and initial conditions group in Table 2 were set to be identical to the inert Case 1 and optimized the remaining constants. The best match of this reduced optimization is shown in blue in Figure 4. The difference between the two optimized solutions arises from fixing 9 of the constants. The optimization is targeted at improving VP and HR, therefore allowing a finer matrix of possible solutions. The ‘final best match’ shows a clear improvement of vapor cloud progression at a small penalty of LP accuracy. The new combustion constants in combination with accurate mixture preparation are observed to produce a good match of Rate of Heat Release (ROHR) and temporal SOC.

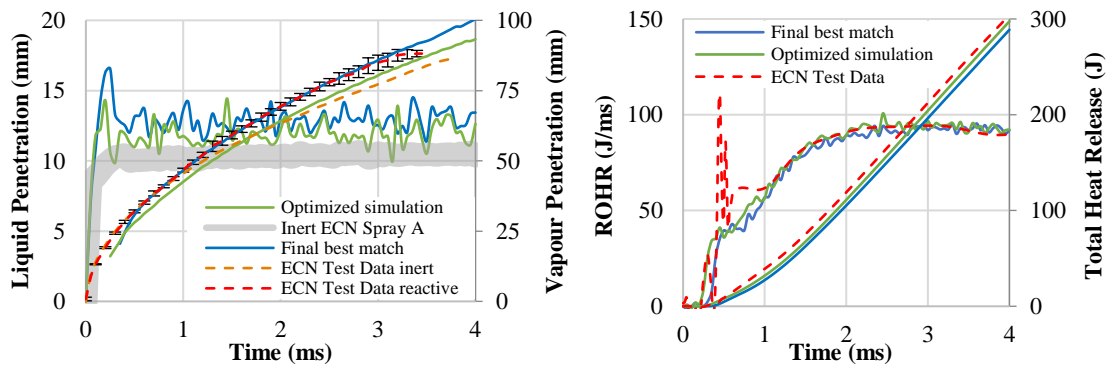


Figure 4: Sim. LP & VP (left) and ROHR & accumulated HR (right) against experimental data

For the reacting Spray A, it is common practice to compare LoL and ignition delay. However, LoL and ignition delay are both based on OH^* chemiluminescence measurements. These metrics cannot be compared because of the use of a simple combustion and ignition model which only uses simple chemical mechanisms and therefore lacks an OH tracking option. As an approximation, a threshold of the RTZF combustion progress variable was defined. SOC was approximated by setting a threshold of the combustion progress variable. Based on this metric, it was found that the spray was igniting about 2mm too early. This combined with the fact that LP was modelled slightly longer than what was measured experimentally for the non-reacting cases, meant that the spray transitioned from evaporation to combustion too rapidly. This suggests that there is still merit for more investigation in this direction. There may be justification to reduce B_1 to speed up primary atomization and increase C_{ig} to delay auto-ignition. The exact combination of constants will be a matter for further research.

Summary and Conclusions

Replicating the complex combustion event in a combustion chamber is a complex task with countless physical processes. The accurate prediction of the atomization process is one of the key elements in the air fuel mixture formation and hence the combustion characteristics and emissions of modern energy systems. From a numerical standpoint, simulating the full spray combustion process from injection to combustion is challenging. One of the major difficulties is that simulation methods such as RANS and LES resolve only part of the scales and thus depend strongly on the accuracy of the SGS models which in turn depend on many tuning coefficients. These coefficients physically encapsulate “unknown” or “unresolved” information at the sub grid scales and thus unrealistic and isolated tuning can lead to compromising the predictive character of the models. In this paper, an integrated Design of Experiments with RANS approach is suggested as a robust and computationally efficient way of providing an optimal set of “tuning constants” for the simulations of a high injection pressure n-dodecane spray (ECN Spray A). The suggested approach, although is implemented in the RANS context in the current paper, can be extended to the LES context in a straightforward manner. The findings in this paper can be summarized as follows:

- The non-reactive simulations performed for a range of injection pressures revealed that conventional spray models designed for moderate injection pressures can capture higher pressure dynamics given appropriate coefficient tuning. Moreover, it was found that a unique set of coefficients that offers very good match in terms of VP and LP for all the cases under investigation exists. This means that

the coefficients used in the inert cases are capable of handling changes in injection pressure. Previous work has shown that this is not the case for changes in charge density.

- This work also offers an insight on how processes usually present in the sub-grid scale like droplet breakup are influenced by changes in injection pressures. The results were counter intuitive as the lower injection pressure case had smaller droplets at an intermediate stage than higher injection pressures. However, closer considerations of evaporation, droplet velocity and droplet drag effects make physical sense because at a later stage the droplets at higher injection pressures were indeed smaller, lining up with common knowledge. Solid experimental data showing the near nozzle droplet breakup is unfortunately not available.

Based on the second part of this work, it is justifiable to tune breakup constants based on inert laboratory conditions. When transferred to reactive cases, these breakup constants may remain unchanged (although there is merit for slight adjustments), while turbulence and combustion settings must be adjusted. The ECN offers a good boundary condition matrix to develop a ‘breakup constant vs condition’ matrix which could in future support a breakup constant input parameter table for more complex calculations of real devices. To expand this ‘input parameter table’ one could incorporate reactive cases by running multiple combusting cases with the same approach as shown in this work. The result of the quantification of these constants would remove the element of tuning, which is one of the largest source of uncertainty in both RANS and LES simulations.

Acknowledgements

The authors would like to acknowledge the support by Kenan Mustafa and Nick Winder from Ricardo Innovations. Further, VECTIS support was provided by Evgeniy Shapiro, Nick Tiney and Irfan Ahmed from Ricardo Software and finally the nCal software assistance provided by Justin Seabrook. The authors would also like to thank the UK’s Engineering and Physical Science Research Council support through the grant EP/P012744/1.

References

- [1] M. Hermann and M. Gorokhovskiz, *Center for Turbulence Research Proceedings of the Summer Program* (Stanford univeristy) **2008**.
- [2] S. Banerjee and C. Rutland in *On LES Grid Criteria for Spray Induced Turbulence*, SAE International, **2012**.
- [3] M. Bolla, M. A. Chishty, E. R. Hawkes and S. Kook, *International Jour. of Engine Research* **2017**, 18, 6-14.
- [4] W. P. Jones and B. E. Launder, *International Journal of Heat and Mass Transfer* **1972**, 15, 301-314.
- [5] D. M. Nsikane, K. Mustafa, A. Ward, R. Morgan, D. Mason and M. Heikal, *SAE Int. J. of Engines* **2017**, 10.
- [6] G. B. L. Pickett, R. Payri in *Engine Combustion Network*, [http:// www.ca.sandia.gov/ecn](http://www.ca.sandia.gov/ecn), **2014**.
- [7] L.-M. Malbec, J. Egúsquiza, G. Bruneaux and M. Meijer, **2013**.
- [8] M. Meijer, B. Somers, J. Johnson, J. Naber, S.-Y. Lee, L. M. Malbec, G. Bruneaux, L. M. Pickett, M. Bardi, R. Payri and T. Bazyn, *Atomization and Sprays* **2012**, 22, 777-806.
- [9] L. M. Pickett, C. L. Genzale, G. Bruneaux, L.-M. Malbec, L. Hermant, C. Christiansen and J. Schramm, *SAE International Journal of Engines* **2010**, 3, 156-181.
- [10] J. Benajes, R. Payri, M. Bardi and P. Martí-Aldaraví, *Applied Thermal Engineering* **2013**, 58, 554-563.
- [11] R. Payri, J. M. García-Oliver, T. Xuan and M. Bardi, *Applied Thermal Engineering* **2015**, 90, 619-629.
- [12] Y. Pei, M. J. Davis, L. M. Pickett and S. Som, *Combustion and Flame* **2015**, 162, 2337-2347.
- [13] A. Aljure, X. Tauzia and A. Maiboom in *Comparison of Eulerian and Lagrangian 1D Models of Diesel Fuel Injection and Combustion*, SAE International, **2017**.
- [14] G. Li, S. M. Sapsford and R. E. Morgan in *CFD Simulation of DI Diesel Truck Engine Combustion Using VECTIS*, SAE International, **2000**.
- [15] A. Putnam in *Integratable Form of Droplet Drag Coefficient*, J. Am. Rocket Soc., **1961**, pp. 1467-4798.
- [16] A. Lefebvre, *Atomization and Sprays*, Taylor & Francis, **1988**, p.
- [17] J. C. Beale, *Modeling fuel injection using Kelvin-Helmholtz/Rayleigh-Taylor hybrid atomization model in KIVA-3V*, University of Wisconsin--Madison, **1999**, p.
- [18] S. D.B. in *The Combustion of Liquid Fuels*, Williams & Wilkins, Baltimore, **1953**, pp. pp. 847-864.
- [19] J. S. a. L. Chin, A.H., *Int. J. Turbo Jet Engines* **1985**, vol. 2., pp. 315-325.
- [20] C. Chen, M. E. A. Bardsley and R. J. R. Johns in *Two-Zone Flamelet Combustion Model*, SAE Int., **2000**.
- [21] M. Metghalchi and J. C. Keck, *Combustion and Flame* **1982**, 48, 191-210.
- [22] Ö. L. Gülder, *Symposium (International) on Combustion* **1991**, 23, 743-750.
- [23] S. Som in *Compilation of Spray A Modeling Efforts*, Argonne National Laboratory, ECN 1 Workshop, **2011**.
- [24] C. J. Aul, W. K. Metcalfe, S. M. Burke, H. J. Curran and E. L. Petersen, *Combustion and Flame* **2013**, 160, 1153-1167.
- [25] L. Cai, S. Kruse, D. Felsmann, C. Thies, K. K. Yalamanchi and H. Pitsch, *Energy & Fuels* **2017**, 5533-5542.
- [26] W. P. Jones, A. J. Marquis and K. Vogiatzaki, *Combustion and Flame* **2014**, 161, 222-239.
- [27] A. Irannejad and F. Jaberri, *International Journal of Multiphase Flow* **2014**, 61, 108-128.
- [28] C. Crua, M. R. Heikal and M. R. Gold, *Fuel* **2015**, 157, 140-150.